

Fault Detection and Diagnosis for Sensor in an Aero-Engine System

Zhen Zhao¹, Yi-gang Sun¹, Jun Zhang²

1. College of Electronics Information and Automation, 2. College of Aerospace Engineering, Civil Aviation University of China, Tianjin 300300, China

Email: zhenzhao0523@gmail.com

Abstract: In modern society, civil plane has become more and more important in people's life. How to ensure safety and reliability of civil plane has attracted more and more attention by many research institutes and researchers. As one of the most important part in the civil plane, how to ensure normal operation of aero-engine becomes particularly important. According to statistics, the sensor fault accounts for more than 80% of the total failures in the aero-engine system. In this paper, an aero-engine model is established according to the operational principle of aero-engine using AMESim software. Secondly, the sensor sub-model in above model is modified to simulate drift failure, bias fault, and pulse fault, and to achieve aero-engine sensors' fault data. After that, sensor fault diagnosis model is built based on principle component analysis. Online detection and diagnosis can be realized using this diagnosis model. Simulation results show that the proposed method is feasible and effective.

Key Words: Sensor; Aero-engine; Fault detection and diagnosis; Principle component analysis

1 INTRODUCTION

In modern society, civil aviation has occupied a particularly important position in people's learn, work, and life. However, the ever increasing need also brings more and more severe safety and reliability requirement, especially after MH370 accident. Therefore, many research institutes and scholars have paid more attention on how to ensure the safety and reliability of the civil plane. As the heart of a civil plane, safety and reliability of an aero-engine system is particularly important for two reasons: one is that most of plane accidents are caused by its aero-engine system, and the other is that any tiny fault may well cause a major aircraft accidents [1]. Furthermore, the operating environment of the aero-engine is always very harsh, high temperature, strong vibration, high EMI, high pressure, and etc. Due to the harsh operating environment, the aero-engine is very prone to failure. According to statistics results supplied by relevant department, the sensor fault accounts for more than 80% of the total faults in the aero-engine system. Considering the abovementioned reason, proposing effective fault detection and diagnosis method for sensor in the aero-engine system will greatly improve reliability and safety of the civil plane, and shows very important theoretical and practical significance.

In the past two decades, lots of researches have been made on sensor fault diagnosis for the aero-engine system. In 1987, analytical redundancy method has been proposed to detect sensor's bias and drift failures, whose performance has been evaluated in a test-bed engine system [2]. In 1998,

an analytical redundancy-based approach is presented for sensor fault detection of a single shaft industrial gas turbine [3]. At the same year, a fuzzy logic based accommodation approach for redundant sensor selection is proposed in [4]. In 1999, a sensor fault detection method using I/O linear models to generate residuals permitting the identification of possible sensor faults [5]. After 2000, types of pattern recognition methods have been introduced to detect and diagnose sensor faults, such as neural network [6-8].

Although QAR can record much sensor data for modern aero-engine, the faulty sensor data is still very rare due to that once a fault happens, some protection measure must be implemented to make sure safety operation of the civil plane. Considering few faulty sensor data, this paper firstly builds an aero-engine model based on AMESim software, which can realize simulation in both normal condition and condition with sensor fault. Then, a statistical analysis method is introduced to realize sensor fault detection and diagnosis. Finally, the proposed statistical based sensor fault detection and diagnosis method is experimented using simulated sensors' data achieved from the aero-engine model.

The rest of this paper is organized as below: The aero-engine model with modified sub-model for sensor is depicted in Section 2. The sensor fault detection and diagnosis method is described in Section 3. In Section 4, the proposed fault detection and diagnosis method is illustrated using simulated sensors' output data. Finally, the conclusions are drawn in Section 5.

2 AERO-ENGINE MODEL

With the rapid development of science and technology, large quantity of operation data (including normal and abnormal data) can be recorded through QAR in modern civil plane. However, from a safety perspective, the whole

This work is supported by the project 973 (Grant No. 2014CB744904), Civil aviation science and technology major projects (Project No. MHRD20130112), Joint Funds of the National Natural Science Foundation of China and Civil Aviation Administration of China Key Project (Grant No. U1533201), the Fundamental Research Funds for the Central Universities (Project No. 3122014C010).

control system must take some protection measure immediately after any fault. Therefore, faulty data are still lack. To present a more feasible sensor fault diagnosis method, this paper builds an aero-engine model using AMESim software, which combines lots of module suitable for dynamic characteristics' simulation, and has been proved to be effective in modeling and simulation of engineering machinery hydraulic system.

2.1 Operation Principle of Aero-Engine

Most of aero-engine in civil aviation is turbofan aero-engine, which consists of fan, low-pressure compressor, high-pressure compressor, combustion chamber, high pressure turbine (driving compressor), low pressure turbine (driving fan), exhaust system, etc., as shown in Fig. 1.

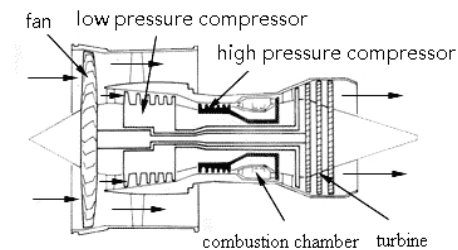


Fig. 1 Structure of a turbofan aero-engine

2.2 Aero-Engine Model

According to the structure of a turbofan aero-engine, the whole model for the turbofan aero-engine in AMESim is modeled as shown in Fig. 2.

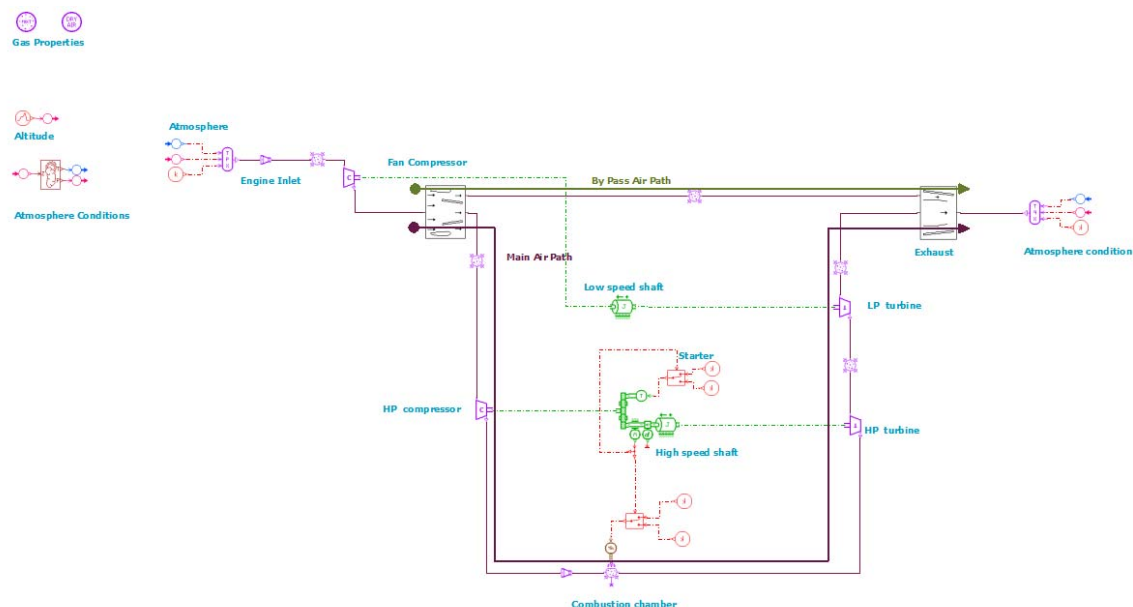


Fig. 2 AMESim model for a turbofan aero-engine

2.3 Sensor Model

In AMESim, it is not able to realize sensor fault simulation through its plug-in module. Thus, it is needed to rebuild appropriate sensor modules or modify the original sensor modules. This paper chooses the second method.

For temperature sensors, firstly, drag the temperature sensor modules from pneumatic components design library, and connect them to low pressure compressor and high pressure compressor in Fig. 2, respectively. Then, add Add controller and Multiply controller to the 2# output port of each temperature sensor. The other input port of each controller can be connected to relevant signal. Finally, sensor fault data can be obtained through the 2# output port of each controller.

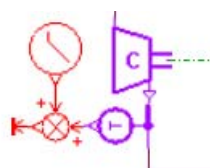


Fig. 3 Temperature sensor for low-pressure compressor

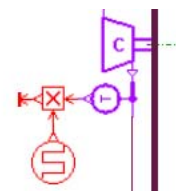


Fig. 4 Temperature sensor for high-pressure compressor

For speed sensors, two speed sensors are dragged from the machine design library, and connected to the low speed shaft and the high speed shaft as shown in Fig. 5 and 6, respectively.

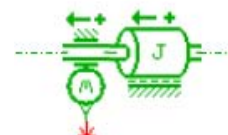


Fig. 5 Speed sensor for low speed shaft

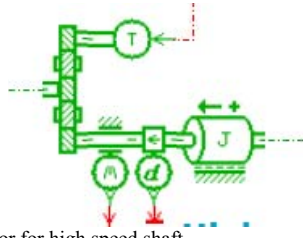


Fig. 6 Speed sensor for high speed shaft

3 SENSOR FAULT DIAGNOSIS in an AERO-ENGINE SYSTEM

A typical statistical analysis method, i.e. principle component analysis (PCA), has been widely applied in many research domain, such as statistical process control, process monitoring, fault detection and diagnosis [1, 8], and so on. To now, PCA have achieved many accomplishments in these fields. So this paper tries to detect and diagnose sensor fault using PCA.

For fault diagnosis, PCA has two phases, i.e. off-line modeling phase and on-line diagnosis phase. On the off-line modeling phase, the normal multi-variables' data is subjected to PCA to build a diagnosis model and get the statistics of T^2 , SPE, and their corresponding control limits. On the on-line diagnosis phase, new coming multi-variables' data is reflected to the diagnosis model to get T^2 statistics or SPE statistics or both. According to the statistics and their corresponding control limits, diagnosis result can be deduced.

3.1 Sensor Diagnosis Model

Given a normal modeling data matrix $X' \in R^{K \times J}$ composed of K samples of J variables (i.e. sensor outputs), which is firstly normalized to a zero-mean and unit-variance matrix $X \in R^{K \times J}$ using Eq. (1).

$$X = [X' - I_m u^T] D_\sigma^{-1/2} \quad (1)$$

where I_m is a $J \times 1$ column vector whose elements are all 1, $u = [u_1, \dots, u_J]^T$ is a mean vector of each variable in X' , $D_\sigma = \text{diag}(\sigma_1^2, \dots, \sigma_J^2)$ is a variance matrix of each variable in X' .

After that, PCA aims to decompose X into

$$X = \hat{X} + \tilde{E} \quad (2)$$

where $T \in R^{K \times l}$ and $P \in R^{J \times l}$ are the score and loading matrices, respectively; E is the residual matrix which can be further decomposed into the product of a residual score matrix \tilde{T} and a residual loading matrix \tilde{P} ; l is the number of principal components (PCs) retained in the statistical model, and is determined using Eq. (3).

$$\sum_{k=1}^i \lambda_k \geq Cl \quad (3)$$

where $\lambda_k (k=1, \dots)$ is the contribution rate of each principle component; $Cl \in [0, 1]$ is threshold of contribution, which is always set to be 95%.

This paper chooses SPE statistics as the monitoring statistics. The SPE statistics can be calculated as bellow:

$$SPE = e_i e_i^T \quad (4)$$

where e_i is the i^{th} row of the residual matrix E , which denotes the residual error at the i^{th} sampling point.

When SPE exceeds its confidence limit Q_α^2 staying for some time, there may be sensor fault. Q_α^2 can be set as below:

$$Q_\alpha = \theta_1 \left[\frac{C_\alpha \bar{2} \bar{\theta}_2 \bar{h}_0^2}{\theta_1} + 1 + \frac{\theta_2 h_0 (h_0 - 1)}{\theta_1^2} \right]^{1/h_0} \quad (5)$$

2.4 On-line Sensor Diagnosis

To realize on-line sensor diagnosis, new sampled data x_{new} can be decomposed using the built diagnosis model as below.

$$x_{\text{new}} = \hat{x}_{\text{new}} + \tilde{x}_{\text{new}} \quad (6)$$

where $\tilde{x}_{\text{new}} = (I - C)x_{\text{new}} = \tilde{C}x_{\text{new}}$, $\hat{x}_{\text{new}} = PP^T x_{\text{new}} = Cx_{\text{new}}$, I is an identity matrix.

Then, the SPE statistics at a new sampling time can be calculated as Eq. (7).

$$\begin{aligned} SPE(x_{\text{new}}) &= \|\tilde{x}_{\text{new}}\|^2 = \tilde{x}_{\text{new}}^T \tilde{x}_{\text{new}} = (I - C)x_{\text{new}}^T (I - C)x_{\text{new}} \\ &= x_{\text{new}}^T (I - P * P^T) x_{\text{new}} \end{aligned} \quad (7)$$

4 ILLUSTRATION AND DISCUSSION

In this section, the proposed statistics based fault detection and diagnosis approach is applied to data obtained from the built aero-engine model. In the model, parameters are set as default. However, simulation time and height is set according to practical flight data. Simulation time is set as 5400s, i.e. 1.5h. Sample period is set as 1s. Height is set as a segmented function in AMESim as shown Fig. 7.

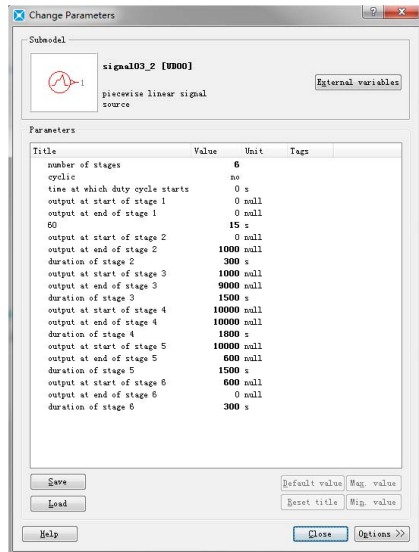


Fig. 7 Flight height setting in AMESim

Figs. 8 and 9 show the temperature, pressure, and speed under normal condition in the aero-engine model. The simulation results are consistent with practical data. However, noise should be added to make the data be nearer with practical data.

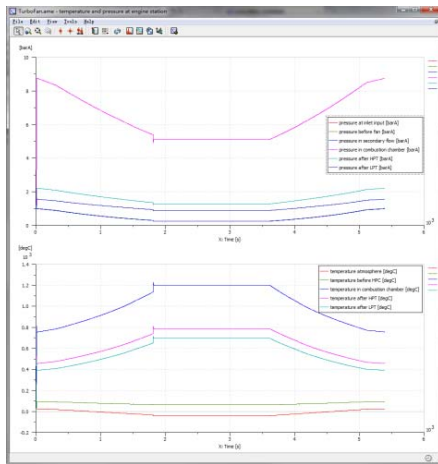


Fig. 8 Temperature and pressure in the aero-engine system

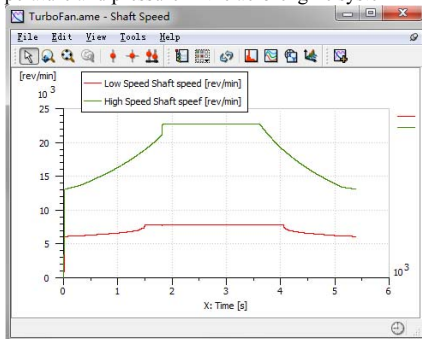


Fig. 9 Speed of the low speed shaft and high speed shaft

Then, four sensors' output data, i.e. FF (Fuel Flow), EGT (Exhaust Gas Temperature), N1 (Low Pressure Rotor Speed), N2 (High Pressure Rotor Speed) and TAT (Total Air Temperature), are recorded under normal and types of fault conditions.

The sampled data is firstly normalized. Using the normal data to build fault detection and diagnosis model, Table 1

shows the contribution rate at off-line modeling stage. The first two principle components' cumulative contribution of variance is 96.63% in Table 1, which is larger than 95%. For this reason, the number of retained PCs is 2, and the control limits are set different at different stage.

Table1. Contribution rate

| Number of principle components | Primary variance contribution rate (%) | Primary cumulative contribution of variance (%) |
|--------------------------------|--|---|
| 1 | 67.11 | 67.11 |
| 2 | 23.51 | 90.62 |
| 3 | 6.01 | 96.63 |
| 4 | 1.76 | 98.39 |
| 5 | 1.61 | 100 |

4.1 No Fault

Fig. 10 shows the SPE statistics under normal condition at on-line stage. From Fig. 10, it can be seen that the SPE statistics is almost under the corresponding control limit, which illustrates that the sensors are all correct.

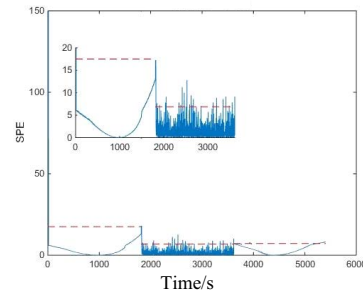


Fig. 10 No fault for temperature sensor of high-pressure compressor (dashed line - control limit, solid line - SPE statistics)

4.2 Drift Bias Fault

A drift bias of 0.005 is added into the temperature sensor for high pressure compressor after the 2700th sampling point. Fig. 11 shows the drift bias fault occurs to the temperature sensor of the high pressure compressor

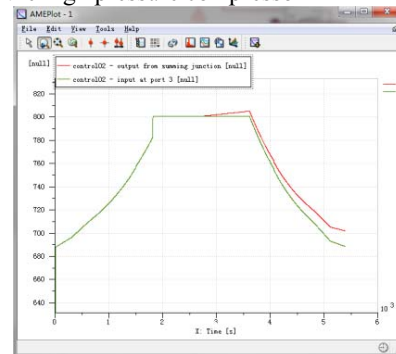
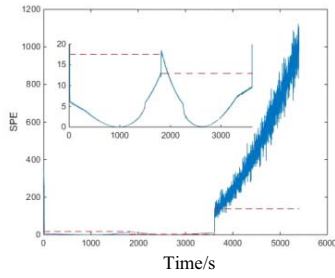
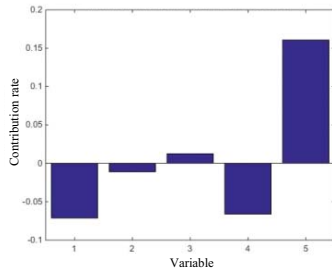


Fig. 11 Drift bias fault of temperature sensor for high pressure compressor Fig. 12 illustrates the diagnosis result for this drift bias fault. From Fig. 12 (a), it can be seen that the SPE statistics exceeds the corresponding control limit at about 3681 sampling point. The reason may be that the drift bias is quite little to be detected by the diagnosis model. Fig. 12 (b) and (c) give the contribution rate histogram at 2800th sampling point and 4000th sampling point, which demonstrates that

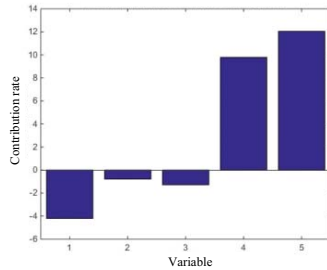
the fifth variable (i.e. temperature sensor output of high pressure compressor) shows largest contribute rate for this phenomenon. This means the temperature sensor of high pressure compressor occurs fault.



(a) SPE statistics



(b) Contribution rate histogram during cruise phase (at 2800)



(c) Contribution rate histogram during landing phase (at 4000)

Fig. 12 Drift bias fault for temperature sensor of high-pressure compressor

4.3 Offset Fault

An offset of 0.05 is added into the temperature sensor of high pressure compressor from the 2700th sampling point. Fig. 13 shows the offset fault occurs to the temperature sensor of high pressure compressor.

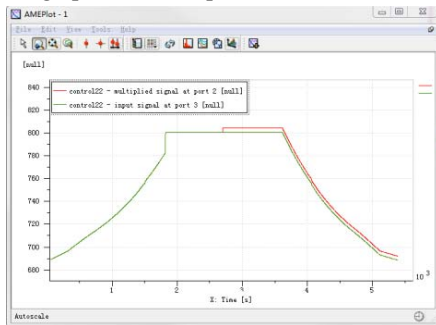
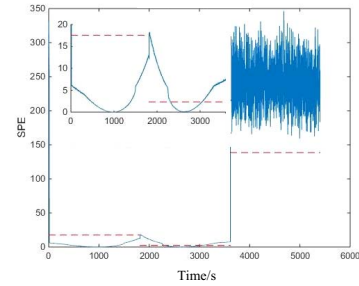


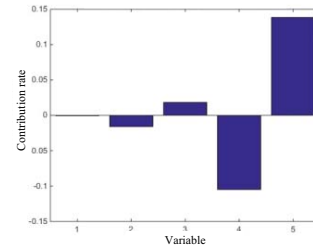
Fig. 13 Offset fault for temperature sensor of high-pressure compressor

Fig. 14 gives the detection and diagnosis results. In Fig. 14 (a), the SPE statistics exceeds its corresponding control limit at about 2700th sampling point. Fig. 14 (b) and (c) shows the contribution rate histogram at 2800th sampling point and 4600th sampling point. From this figure, it

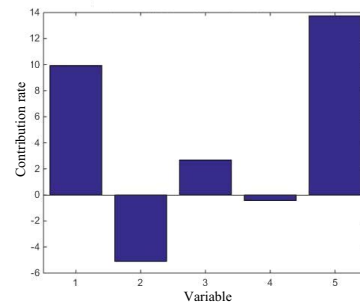
demonstrates that the fifth variable (i.e. temperature sensor output of high pressure compressor) shows largest contribute rate for this phenomenon, which means that the temperature sensor of high pressure compressor occurs fault.



(a) SPE statistics



(b) Contribution rate histogram during cruise phase (at 2800)



(c) Contribution rate histogram during landing phase (at 4600)

Fig. 14 Offset fault for temperature sensor of high-pressure compressor

4.4 Pulse Fault

Pulse fault is similar to offset fault. In this simulation, pulse fault is added into the temperature sensor from the 2700th sampling point. Fig. 15 shows the pulse fault occurs to the temperature sensor of high pressure compressor.

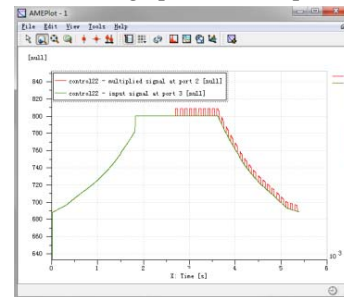
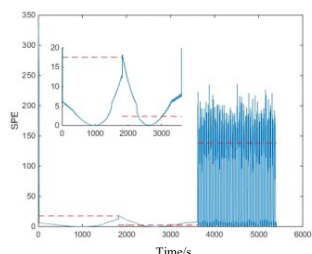


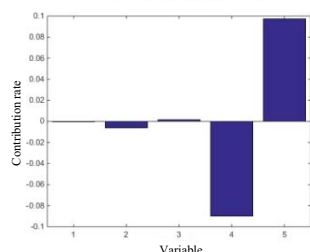
Fig. 15 Pulse fault for temperature sensor of high-pressure compressor

Fig. 16 (a) shows the SPE statistics for pulse fault, Fig. 16 (b) and (c) illustrates the contribution rate histogram at the 2800th and 4600th sampling point. From Fig. 16 (a), it can be

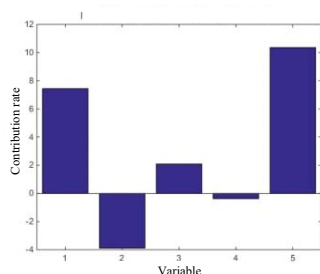
seen that the SPE statistics exceeds its corresponding control limit at about the 3000th sampling point. Fig. 16 (b) and (c) demonstrate that the fifth variable (i.e. temperature sensor output of high pressure compressor) shows largest contribution rate for this phenomenon. This means the temperature sensor output of high pressure compressor occurs fault. The detection and diagnosis result conforms to the set.



(a) SPE statistics (dash line – control limit, solid line – SPE statistics)



(b) Contribution rate histogram during cruise phase (at 2800)



(c) Contribution rate histogram during landing phase (at 4600)

Fig. 16 Pulse fault for temperature sensor of high-pressure compressor

5 CONCLUSION

In this paper, an aero-engine model is firstly modelled using the AMESim software according to the principle of aero-engine model. After that, a statistics based fault detection and diagnosis method is introduced through principle component analysis. On the diagnosis process,

normal data obtained from the built aero-engine model is used to build the off-line diagnosis model. Some types of sensor faults, such as drift bias fault, offset fault and pulse fault, are used to test the detection and diagnosis model. Simulation results show the feasibility and effectiveness of the proposed detection and diagnosis method in the aero-engine system.

REFERENCES

- [1] Zhen Zhao, Yi-gang Sun, Jun Zhang, "PCA-Based Sensor Fault Diagnosis for Aero-Engine," 2015 CCDC, 2015, 2679-2683.
- [2] W. C. Merrill, J. C. DeLaat, and W. M. Bruton, "Advanced detection, isolation, and accommodation of sensor failures real-time evaluation," NASA, pp. 1-27, 1987.9.
- [3] S. Simani, P. Spina, S. Beghelli, R. Bettocchi, and C. Fantuzzi, "Fault detection and isolation based on dynamic observers applied to gas turbine control sensors," ASME, 1998.
- [4] T. Healy, L. Kerr, and L. Larkin, "Model based fuzzy logic sensor fault accommodation," Journal of Engineering for Gas Turbines and Power, vol. 120, pp. 533-536, 1998.
- [5] N. Aretakis, K. Mathioudakis, and A. Stamatis, "Identification of sensor faults on turbofan engines using pattern recognition techniques," Control Engineering Practice, vol. 12, pp. 827-836, 2004.
- [6] M. Napolitano, A. Younghwan, and B. Seanor, "A fault tolerant flight control system for sensor and actuator failures using neural networks," Aircraft Design, vol. 3, pp. 103-128, 2000.
- [7] K. Botros, G. Kibrya, and A. Glover, "A demonstration of artificial neural networks based data mining for gas turbine driven compressor stations," ASME, vol. 3, pp. 2000-GT-0351, 2000.
- [8] P. Dewallef and O. Leonard, "On-line validation of measurements on jet engines using automatic learning methods," ISABE, pp. 2001-1031, 2001.
- [9] Zhao Chunhui, Wang Fuli, Lu Ningyun, Jia Mingxing. Stage-based Soft-transition Multiplepca Modeling and On-line Monitoring Strategy for batch processes [J], Journal of Process Control, 2007, 17(9): 728-741.
- [10] Yue, H. Henry, Qin, S. Joe. Reconstruction-based fault identification using a combined index [J], Industrial & Engineering Chemistry Research, 2001, 40(20): 4403-4414.